

10/25/92 85①  
3-2

LBL-31272  
UC-406



# Lawrence Berkeley Laboratory

UNIVERSITY OF CALIFORNIA

## Engineering Division

### Some Recent Silicon Detector Spectroscopy Applications at the Lawrence Berkeley Laboratory

J.T. Walton

October 1990



Prepared for the U.S. Department of Energy under Contract Number DE-AC03-76SF00098

## DISCLAIMER

This document was prepared as an account of work sponsored by the United States Government. Neither the United States Government nor any agency thereof, nor The Regents of the University of California, nor any of their employees, makes any warranty, express or implied, or assumes any legal liability or responsibility for the accuracy, completeness, or usefulness of any information, apparatus, product, or process disclosed, or represents that its use would not infringe privately owned rights. Reference herein to any specific commercial product, process, or service by its trade name, trademark, manufacturer, or otherwise, does not necessarily constitute or imply its endorsement, recommendation, or favoring by the United States Government or any agency thereof, or The Regents of the University of California. The views and opinions of authors expressed herein do not necessarily state or reflect those of the United States Government or any agency thereof or The Regents of the University of California and shall not be used for advertising or product endorsement purposes.

**This report has been reproduced directly  
from the best available copy.**

**Available to DOE and DOE Contractors  
from the Office of Scientific and Technical Information  
P.O. Box 62, Oak Ridge, TN 37831  
Prices available from (615) 576-8401, FTS 626-8401**

**Available to the public from the  
National Technical Information Service  
U.S. Department of Commerce  
5285 Port Royal Road, Springfield, VA 22161**

Lawrence Berkeley Laboratory is an equal opportunity employer.

LBL--31272

DE92 009490

## **Some Recent Silicon Detector Spectroscopy Applications at the Lawrence Berkeley Laboratory**

J.T. Walton  
Engineering Science Department, Engineering Division  
Lawrence Berkeley Laboratory,  
University of California, Berkeley, CA 94720

October 1990

This work was supported by the Director, Office of Energy Research,  
Office of Health and Environmental Research, U.S. Department of Energy  
under contract DE-AC03-76SF00098.

MASTER

80

# SOME RECENT SILICON DETECTOR SPECTROSCOPY APPLICATIONS AT THE LAWRENCE BERKELEY LABORATORY

J. T. Walton  
Engineering Science Department, Engineering Division  
Lawrence Berkeley Laboratory  
University of California, Berkeley, CA 94720

## Abstract

The development and fabrication of specialized silicon detectors have long been an integral part of the LBL experimental capabilities. This silicon detector expertise utilizes two basic technologies, oxide-passivated diffused junction and lithium-ion drift. These technologies are complementary, with detectors of 10  $\mu\text{m}$  to 500  $\mu\text{m}$  thick fabricated using the diffused junction process and detectors 500  $\mu\text{m}$  to 10,000  $\mu\text{m}$  using the lithium-ion technique. Particle spectroscopy applications at LBL typically employ a thin diffused, dE/dx, detector followed by a thick lithium drifted, E, detector. Novel position-sensitive dE/dx and E detectors recently employed in two separate experiments conducted at LBL are described. In addition, the requirements for employing thick lithium drifted detectors in an ongoing LBL double beta decay experiment and a LBL dark matter search are also presented.

## Introduction

The Lawrence Berkeley Laboratory (LBL) has for over thirty years maintained staff and facilities to develop and provide specialized semiconductor radiation detectors often required for novel experiments conducted at the Laboratory or elsewhere. For silicon radiation detectors, experimental requirements led, very early, to the adoption of two fabrication technologies—oxide passivated diffused junction<sup>1</sup> and lithium-ion drift.<sup>2</sup> We are still are still using these technologies today to provide an ever-widening array of silicon detectors for spectroscopy applications.

Good descriptions of semiconductor p-n junction radiation detectors are in the literature.<sup>3-5</sup> Figure 1 illustrates a few basic concepts that are needed in the following discussion. As noted in this figure, the detector depletion depth depends on the applied bias and semiconductor impurity concentration. This dependence of the depletion depth on impurity concentration for p-type silicon is shown further in Fig. 2.

Presently, high purity poly-silicon ingots, from which the silicon single crystals are grown by the float-zone process, can be obtained with impurity concentrations of 0.004 to 0.06 ppb.<sup>6</sup> Consequently from Fig. 2 it can be seen that, with these silicon purification limits, the maximum detector depletion depth is restricted to about 1 – 2 mm. This thickness limitation, if real, would greatly reduce the possible applications for silicon radiation detectors. However, by using the lithium ion drift process, it is possible to reduce substantially the net acceptor concentration, thereby making feasible thicker silicon detectors.

Lithium is an interstitial donor that pairs with acceptor ions present in silicon to form lithium-acceptor ion pairs that are electrically neutral. As indicated in Fig. 2, the net acceptor concentration in a silicon crystal can be lowered to about  $0.5 - 1.0 \times 10^{10}$  acceptors/cm<sup>3</sup> by this pairing process. This low net acceptor impurity concentration allows the fabrication of detectors with depletion depths of 10 mm or more.

The two technologies in use at LBL are therefore complementary. Detectors 10  $\mu\text{m}$  to 500  $\mu\text{m}$  thick are fabricated on high purity silicon with a diffused junction process. Detectors 500  $\mu\text{m}$  to 10,000  $\mu\text{m}$  are fabricated on lithium ion drifted silicon with a silicon lithium drift process. We discuss further in the next section the characteristics of these two detector types.

### LBL Silicon Detector Characteristics

Figure 3 shows schematically the basic LBL silicon lithium ion drifted [Si(Li)] and silicon diffused junction detectors. While we use p-type silicon with both of these detector types, our processing sequence is different, resulting in different detector design parameters and final characteristics.

We fabricate Si(Li) detectors using low temperature processing. The n+ contact is formed by diffusing at 375° C lithium into the silicon wafer. The subsequent lithium ion drift is performed at 120° C.<sup>7</sup> These detectors are not very tolerant to high temperature excursions after fabrication as lithium is quite mobile in silicon. Even prolonged storage at room temperature can cause the lithium-acceptor pairs to dissociate and the lithium n+ contact thickness to increase.<sup>8</sup> However, "old" detectors can be reprocessed to reestablish the lithium-acceptor pairing or to repair radiation damage. Radiation damage often appears as an acceptor center in silicon<sup>9</sup> and by redrifting these "acceptor" centers can be partially compensated. We have made these detectors in a wide range of geometrical shapes including conical and coaxial. In addition, we have produced single and double-sided position sensitive Si(Li) detectors<sup>10</sup> and pixel designs.<sup>11</sup> We summarize in Table 1 our present capabilities with these detectors.

Table 1. Si(Li) Detector Capabilities

Detector Diam.	Detector Thick.	N+ Contact Thick.	P+ Contact Thick.
2 - 100 mm	0.5 - 10 mm	5 - 35 mgm/cm <sup>2</sup>	10 - 40 $\mu\text{gm}/\text{cm}^2$

For the diffused junction detectors we use high temperature processing. We grow the passivating oxide at 1000° C, and form the n+ contact with a phosphorus diffusion at 950° C.<sup>12</sup> Typically we use a boron implantation to make the p+ contact and anneal this implantation at 800° C. These diffused junction detectors are quite rugged and can survive extensive periods at elevated temperatures. However, unlike the Si(Li) detectors, there is no inherent compensation process available with these to correct radiation damage effects. Radiation damage can be repaired by annealing at 500 - 800° C, but often this is impractical due to the detector packaging and/or the presence of metal contacts. Again, we have made these diffused junction detectors in a wide array of geometrical shapes. Further, since we can pattern the oxide using photolithographic

techniques, diverse geometrical patterns are possible. Although we have made double sided position sensitive diffused junction detectors, we normally make these detectors position sensitive on only one side. Signals present on each side of a double sided thin position sensitive detector often interact which can limit the detector's usefulness.<sup>13</sup> We tabulate in Table 2 our present capabilities with these devices.

**Table 2. Diffused Junction Detector Capabilities**

Detector Diam.	Detector Thick.	N+ Contact Thick.	P+ Contact Thick.
0.1 - 75 mm	10 - 500 $\mu\text{m}$	100 $\mu\text{gm}/\text{cm}^2$	60 $\mu\text{gm}/\text{cm}^2$

Both detector types have been used by experimental groups at LBL and elsewhere in a wide array of experiments. We discuss a few of these applications in the next section.

### **LBL Silicon Detector Applications**

A common spectroscopy application using both thin and thick silicon detectors is in particle identifier telescopes where the signal from the thin detector is proportional to the particle's rate of energy loss,  $dE/dx$ , while the signal from the thick detector is proportional to the particle's energy,  $E$ . Knowing  $dE/dx$  and  $E$ , it is possible to identify a wide range of particles with a high degree of precision.<sup>14</sup> In applications where the particle trajectories are angularly dispersed, position sensitive  $dE/dx$  and  $E$  detectors in the telescope can be used to determine the trajectories and thereby extend the telescope's range and precision.

In a series of experiments characterizing heavy ion projectile breakup reactions, W.D. Rae has used a variety of LBL fabricated position sensitive  $dE/dx$  and  $E$  detectors in his particle identifiers.<sup>15</sup> The inclusion of position sensitive detectors in these particle identifiers permitted the use of wide solid angles (10 - 15°) in these experiments while maintaining the required particle identification capabilities. The characteristics of the most recent detectors employed in these experiments are listed in Table 3 while the detectors and packaging are shown in Fig. 4.

**Table 3. Heavy Ion Projectile Breakup Reaction Detectors<sup>15</sup>**

Detector	Thickness	Active Area	Typical Resolution at 1.6 $\mu\text{sec}$	
			Energy	Position
$dE/dx$	20 - 40 $\mu\text{m}$	11 x 11 mm	25 keV	100 keV
$E$	3 - 5 mm	11 x 11 mm	60 keV	100 keV

A second example of a particle identifier using position sensitive detectors is the detector array that G. Wozniak has employed to identify heavy ion fragments produced by reverse kinematics reactions.<sup>16</sup> The LBL fabricated array detectors, 300  $\mu\text{m}$  and 5000  $\mu\text{m}$  thick, have position sensing contacts that are segmented into a series of high

and low conductivity strips. The position signal from these detectors therefore has discrete levels, which simplifies calibration of the detector linearity and facilitates on-line monitoring of the detector performance. Figure 5 shows the detectors and packaging. The detectors are mounted in the array so that the high conductivity strips on the E detector, visible in the figure, are orthogonal to those on the dE/dx detector. The detector characteristics are summarized in Table 4.

**Table 4. Heavy Ion Fragment Detectors<sup>16</sup>**

Detector	Thickness	Active Area	Typical Resolution at 1.6 $\mu$ sec	
			Energy	Position
dE/dx	~300 $\mu$ m	44.8 x 44.8 mm	80 keV	150 keV
E	~5000 $\mu$ m	44.8 x 44.8 mm	60 keV	100 keV

Figure 6 shows a comparison of the particle spectrum with and without trajectory correction. The improvement obtained in particle identification with trajectory correction is evident in this figure.

Besides the particle identifier detectors, we have, in the past several years, fabricated Si(Li) detectors for several neutrino mass experiments. One of these experiments, the neutrinoless double beta decay of  $^{100}\text{Mo}$ , employs a stack of Si(Li) detectors interleaved with the  $^{100}\text{Mo}$  foils shown schematically in Fig. 7. These Si(Li) detectors are 7.6 cm in diameter, 0.14 cm thick and are separated from each other by a gap of 0.1 cm into which the  $^{100}\text{Mo}$  foils are inserted.<sup>17</sup> To improve the energy resolution and background rejection capabilities of this experiment, we fabricated the Si(Li) detectors so that the entrance window thickness for both the n+ and p+ contacts were negligible (~20  $\mu\text{gm}/\text{cm}^2$  for the n+ and 40  $\mu\text{gm}/\text{cm}^2$  for the p+). The detector fabrication procedure is outlined in Fig. 8.

These neutrino mass and other searches for dark matter<sup>18</sup> are critically dependent on minimizing extraneous radioactive contamination in the experimental apparatus. Also of concern is the presence in the silicon detectors of radionuclei that are beta emitters producing a continuum over the energy range in which spectral lines are expected.

As indicated in our discussion of Fig. 2, high purity silicon, as used in silicon detector fabrication, typically has contaminants in the sub-ppb range and these are mainly light elements (A < 26). Review of the "Table of Isotopes"<sup>19</sup> yields only three light element isotopes that produce a beta continuum. These are listed in Table 5. Both the  $^{32}\text{Si}$  and  $^{42}\text{Ar}$  decays involve second radionuclei which are noted in brackets in the table.

**Table 5. Possible Radionuclei Present in High Purity Silicon**

Isotope	Half Life	Beta Endpoint
$^3\text{H}$	12.2 y	0.018 MeV
$^{32}\text{Si}$ (32P)	133 y (14.3 d)	0.21 (1.71) MeV
$^{42}\text{Ar}$ (42K)	33 y (12.4 h)	0.60 (3.5) MeV

While high purity silicon crystals are typically grown in Argon using the float zone process, the Argon solubility in silicon at the processing temperature ( $\sim 1400^\circ \text{C}$ ) is small and therefore  $^{42}\text{Ar}$  should not be present in detectable quantities. However,  $^3\text{H}$  and  $^{32}\text{Si}$  are probably present in most silicon crystals and in fact were unambiguously identified<sup>20</sup> as contributing at one point to the observed background in LBL-Santa Barbara  $^{76}\text{Ge}$  neutrino mass experiment where silicon is part of the cryostat mechanics.<sup>21</sup>

Both  $^3\text{H}$  and  $^{32}\text{Si}$  are introduced into a silicon crystal by cosmic rays—but at different points in the crystal's history. The radionuclide  $^{32}\text{Si}$  results from the interaction of cosmic rays with atmospheric argon nuclei with its subsequent deposition on the earth's surface. For samples on the earth's surface ratios of  $^{32}\text{Si}$  to the stable silicon isotopes of  $10^{-15}$  to  $10^{-17}$  are reported.<sup>22</sup> Since normally there are no processing steps in the production of the silicon crystals that will separate the  $^{32}\text{Si}$  from the stable silicon isotopes, minimizing the  $^{32}\text{Si}$  concentration in the final crystal requires minimizing its presence in the starting polysilicon.

In contrast,  $^3\text{H}$  is introduced into the crystal by cosmic rays after the crystal is grown. As noted earlier, FZ crystals are typically grown in an argon atmosphere with the crystal at about  $1400^\circ \text{C}$ . Therefore  $^3\text{H}$  should not be present in the initially grown crystal, but should result from the subsequent stopping of cosmic rays in the crystal.

For detectors to be used in dark matter searches, we therefore have been exploring with various FZ silicon vendors the possibility of obtaining crystals grown from poly material that was refined from silica deep in the ground (to minimize the  $^{32}\text{Si}$  concentration) and then transported via land or sea (to minimize the  $^3\text{H}$  concentration).

## Discussion

The semiconductor group at LBL has had a long history of collaborative agreements with the experimental community, both at LBL and elsewhere, that have often led to innovative advances in detector technology. We have briefly summarized the present state of these advances in silicon detector technology at LBL and have given a few examples where experiments have directly benefitted from our collaborative involvement.

## Acknowledgements

Discussions with members of the various experimental groups mentioned in this report are gratefully acknowledged. In addition, discussions with Dr. F.S. Goulding on various detector topics, especially on the presence of beta emitters in silicon, are also gratefully acknowledged. This work was supported by the Director's Office of Energy Research, the Office of Health and Environmental Research, and the U.S. Department of Energy under contract No. DE-AC03-76SF00098.

## References

1. F.S. Goulding and W.L Hansen, "Leakage Current in Semiconductor Junction Radiation Detectors and Its Influence on Energy Resolution Characteristics," *Nucl. Inst. and Methods* **12**, 249 (1961).
2. J.N. Elliot, "Thick Junction Radiation Detectors Made by Ion Drift," *Nucl. Inst. and Methods* **12**, 249 (1961).
3. G. Bertolini and A. Coche, Eds., Semiconductor Detectors, Elsevier-North Holland, Amsterdam (1968).
4. G.F. Knoll, Radiation Detection and Measurement, John Wiley and Sons, New York (1987).
5. S. Middlehoeck and S.A. Audet, Silicon Sensors, Academic Press, San Diego (1989).
6. Symposium on High Purity and High Resistivity Silicon, The Electrochemical Society, Seattle, WA, October 17, 1990.
7. D.A. Landis, Y.K. Wong, J.T. Walton and F.S. Goulding, "Computer Controlled Drifting of Si(Li) Detectors," *IEEE Trans. Nucl. Sci.* **NS-36**, No.1, 185 (1989).
8. J.T. Walton, R.H. Pehl, Y.K. Wong and C.P. Cork, "Si(Li) X-Ray Detectors with Amorphous Silicon Passivation," *IEEE Trans. Nucl. Sci.* **NS-31**, No.1, 331 (1984).
9. H.W. Kraner, "Radiation Damage in Semiconductor Detectors," *IEEE Trans. Nucl. Sci.* **NS-29**, 1088 (1987).
10. J.T. Walton, G.S. Hubbard, E.E. Haller and H.A. Sommer, "A Two-Dimensional Position Sensitive Si(Li) Detector," *IEEE Trans. Nucl. Sci.* **NS-26**, No.1, 334 (1979).
11. A.C. Thompson, H. Zeeman, W. Thomlinson, E. Rubenstein, R.S. Kernoff, R. Hofstadter, J.C. Giacomini, H.J. Gordon, and G.S. Brown, "Imaging of Coronary Arteries Using Synchrotron Radiation," *Nucl. Inst. and Methods* **B40/41**, 407 (1989).
12. J.T. Walton and F.S. Goulding, "Silicon Radiation Detectors with Oxide Charge State Compensation," *IEEE Trans. Nucl. Sci.* **NS-34**, No.1, 396 (1987).
13. A.J. Tuzzolino, "Two-Dimensional Position Sensing Si Detectors: Current and Charge Pulse Characteristics," *Nucl. Inst. and Methods* **A270**, 157 (1988).
14. F.S. Goulding and B.G. Harvey, *Annual Review of Nuclear Science* **25**, 167 (1975).

15. B.R. Fulton, S.J. Bennett, M Freer, R.D. Page, P.J. Woods, S.C. Allcock, A.E. Smith, W.D.M. Rae and J.S. Lilley, *Phys. Lett. B* **232**, No.1, 56 (1989).
16. J.T. Walton, H.A. Sommer, G.J. Wozniak, G.F. Peaslee, D.R. Bowman, W.L. Kehoe and A. Moroni, "Self Calibrating Position Sensitive Detectors," *IEEE Trans. Nucl. Sci.* **NS-37**, No.5, 1578 (1990).
17. M. Alston-Garnjost, B.L. Dougherty, R.W. Kenney, R.D. Tripp, J.M. Krivicich, H.W. Nicholson, C.S. Sutton, B.D. Dieterle, S.D. Foltz, J. Kang, C.P. Leavitt, R.A. Reeder, J.D. Baker, and A.J. Caffrey, "Search for Neutrinoless Double-B Decay of  $^{100}\text{Mo}$ ," *Phys. Rev. Letters* **63**, No.16, 1671 (1989).
18. B. Sadoulet, J. Rich, M. Spiro, and D.O. Caldwell, "Testing the Weakly Interacting Massive Particle Explanation of the Solar Neutrino Puzzle with Conventional Silicon Detectors," *The Astrophysical Journal* **324**, L75 (1988).
19. C.M Lederman, J.M. Hollander, I. Perlman, Table of Isotopes, Sixth Edition, John Wiley and Sons, New York (1967).
20. F.S. Goulding, unpublished results.
21. F.S. Goulding, D.A Landis, P.N. Luke, N.W. Madden, D.F. Malone, R.H. Pehl, and A.R. Smith, "Semiconductor Detectors and Double Beta Decay," *IEEE Trans. Nucl. Sci.* **NS-31**, No. 1, 285 (1984)
22. M.S. Thomsen, J. Heinermeier, P. Hornshoj, H.L. Nielsen, and N. Rud, "Accelerator Mass Spectrometry Applied to  $^{32}\text{Si}$ ," *Nucl. Inst. and Meth.* **B31**, 425 (1988).

## Figure Captions

- Figure 1** A schematic representation of a semiconductor radiation detector. The applied bias,  $V$ , produces a region free of mobile carriers—a depletion region. Incident radiation creates electrons and holes in this depletion region. These electrons and holes are swept by the electric field,  $E$ , to the  $n^+$  or  $p^+$  contacts respectively for subsequent detection by an electronic amplifier.
- Figure 2** As noted in Figure 1, the depletion region is dependent both on the applied bias and the net impurity concentration in the crystal. Here the depletion depth dependence is shown as a function of the impurity concentration in  $p$ -type silicon crystals. Also noted in this figure are representative impurity ranges for lithium-ion drifted silicon, polycrystalline silicon, floating-zone (FZ) silicon, and Czochralski (CZ) silicon.
- Figure 3** The silicon lithium drifted [Si(Li)] detectors fabricated at LBL are a grooved design. This groove serves to define the active area of the device, to assist in the actual fabrication of the device and to sustain the high voltage normally present on these devices. The diffused junction detectors are actually fabricated using both diffusion and ion implantation to form the  $n^+$  (phosphorous) and  $p^+$  (boron) contacts, respectively.
- Figure 4** The diffused junction,  $dE/dx$  and Si(Li),  $E$ , detectors used by W.D. Rae.<sup>15</sup>
- Figure 5** The diffused junction,  $dE/dx$ , and Si(Li),  $E$ , detectors used by G. Wozniak.<sup>16</sup> The high and low conductivity strips that provide the discrete position signal levels are evident on the  $E$  detector in this figure.
- Figure 6** A comparison of the heavy ion fragmentation identification with (A) and without (B) trajectory correction. By knowing the particle's trajectory, its specific energy loss can be calculated, which in turn leads to a better identification of its atomic number,  $Z$ . The large peak in the figure at  $Z = 57$  is the La beam.
- Figure 7** A schematic representation of the stacking arrangement of the Si(Li) detectors and  $^{100}\text{Mo}$  foils used in the LBL  $^{100}\text{Mo}$  neutrinoless double beta decay experiment.<sup>17</sup>
- Figure 8** A simplified fabrication procedure for the  $^{100}\text{Mo}$  Si(Li) detectors. First a Li contact with a ring structure as shown in (A) is diffused into the wafer with a two step diffusion procedure. Second, the detector is then lithium ion drifted (B). Finally, the Li contact in the central region is removed and an aluminum metal contact is evaporated onto this surface (C).

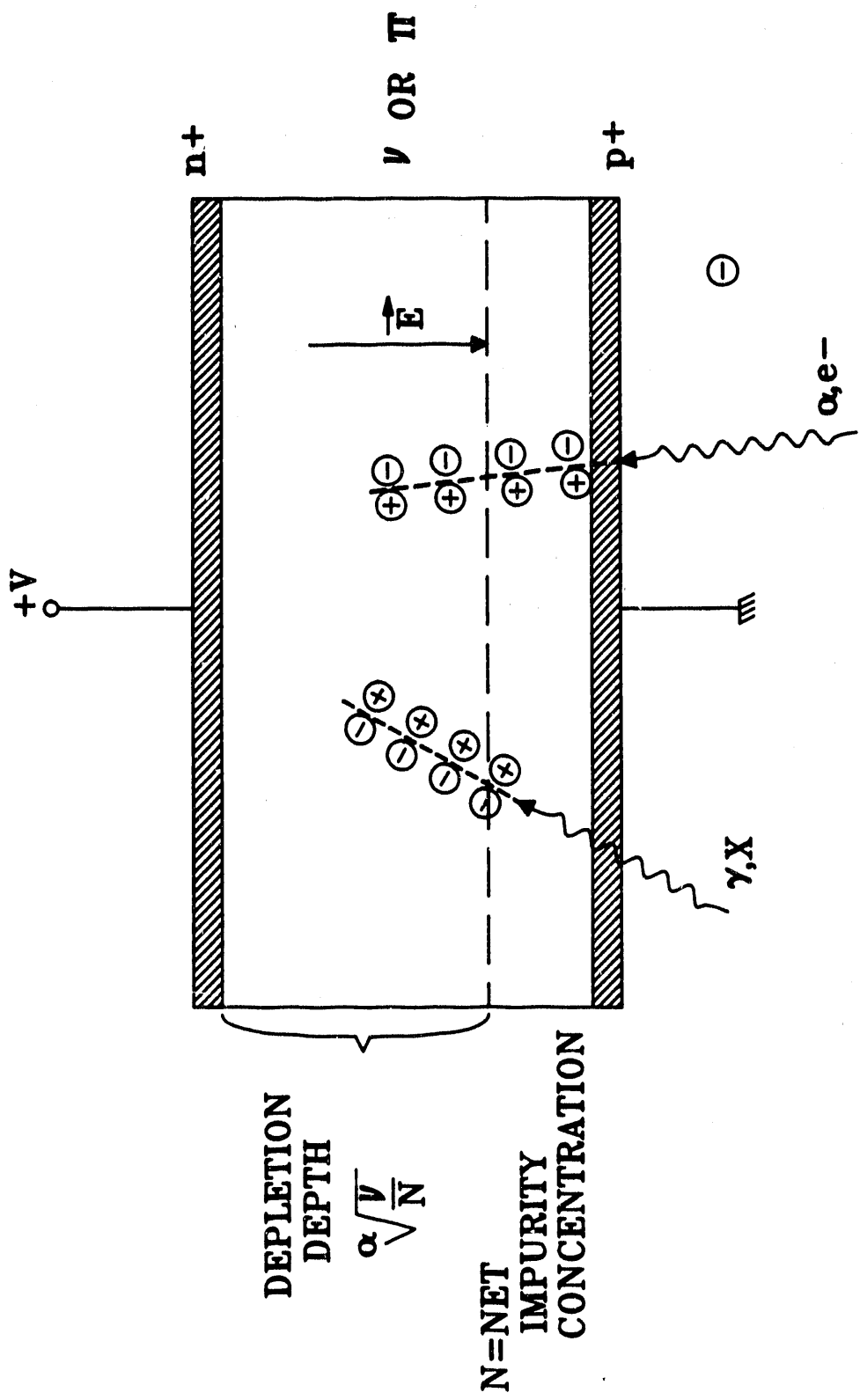


Figure 1

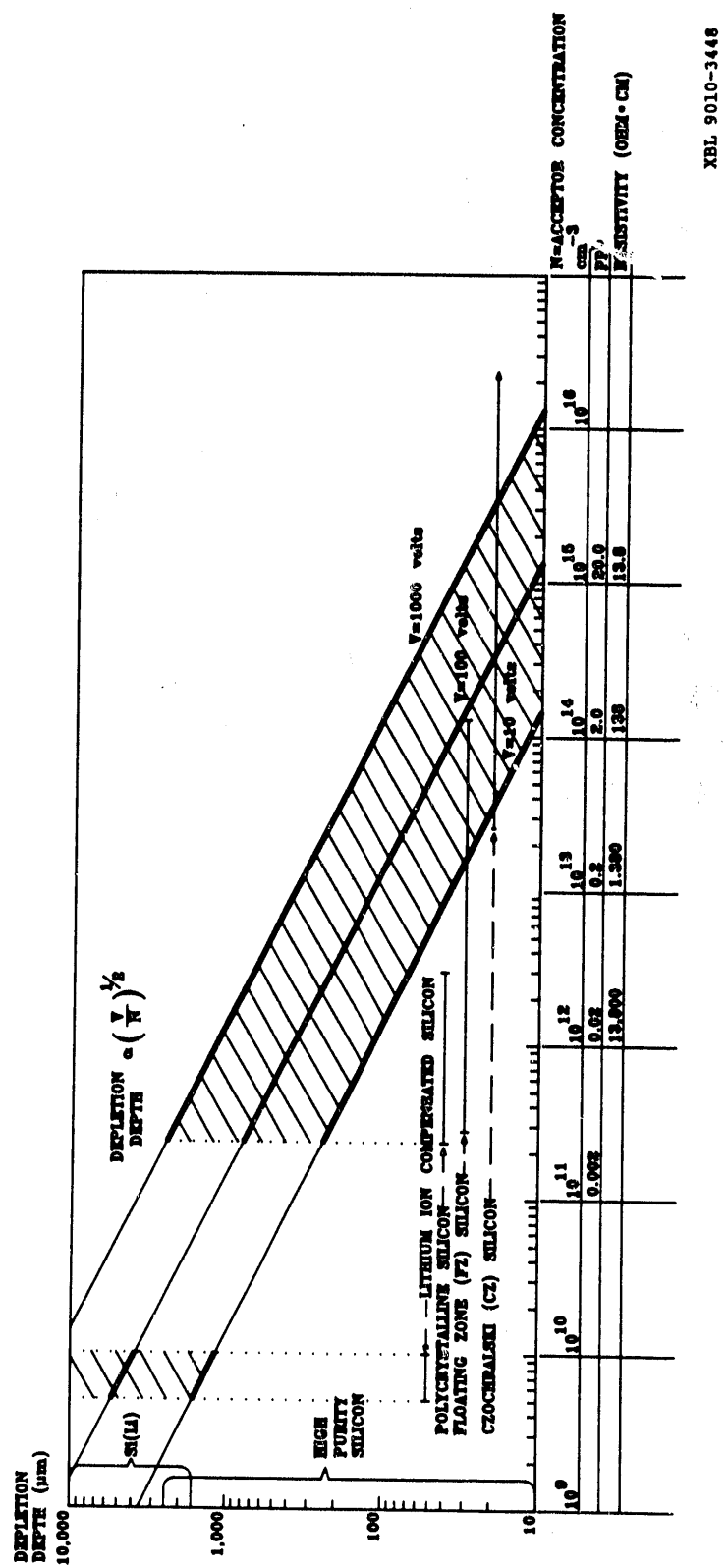
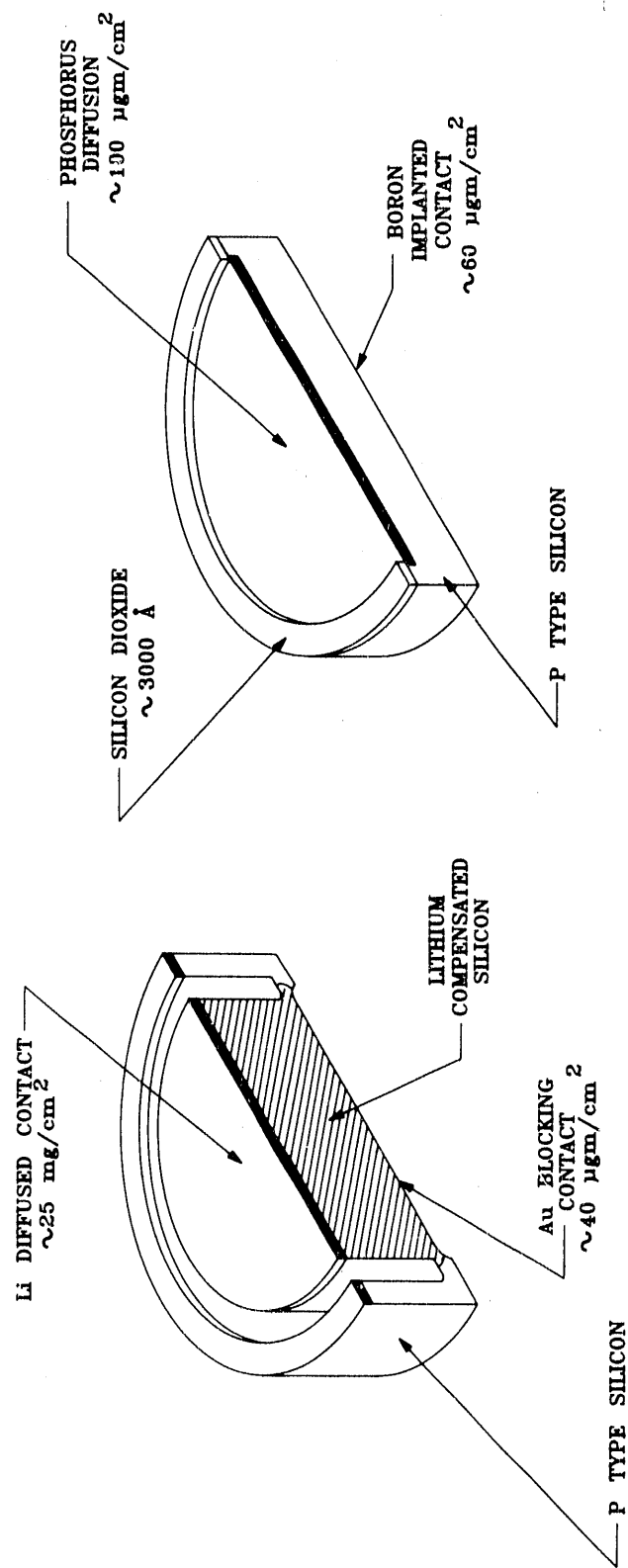


Figure 2

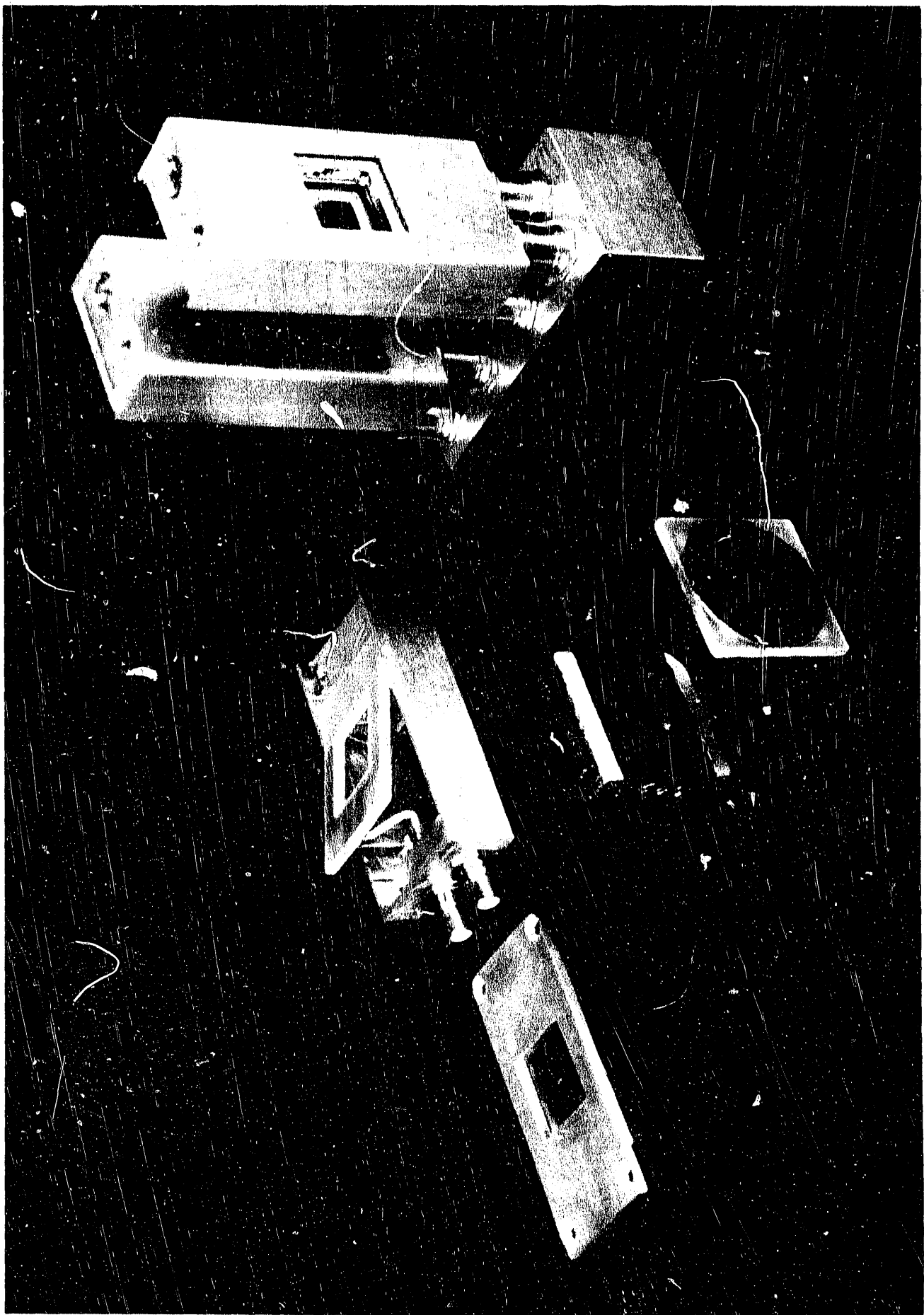


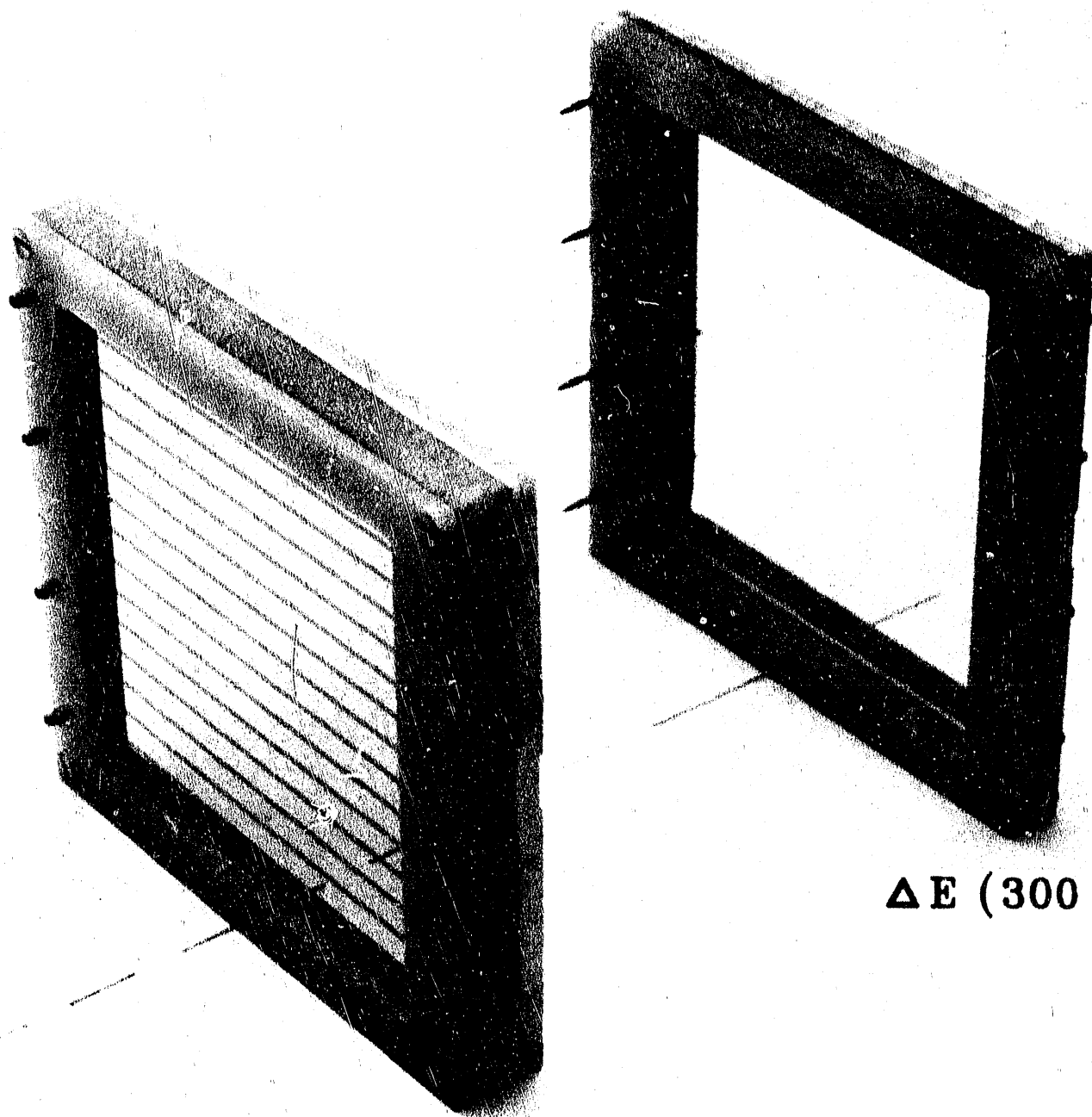
XBL 9010-3447

Figure 3

CBB 900-8301

Figure 4



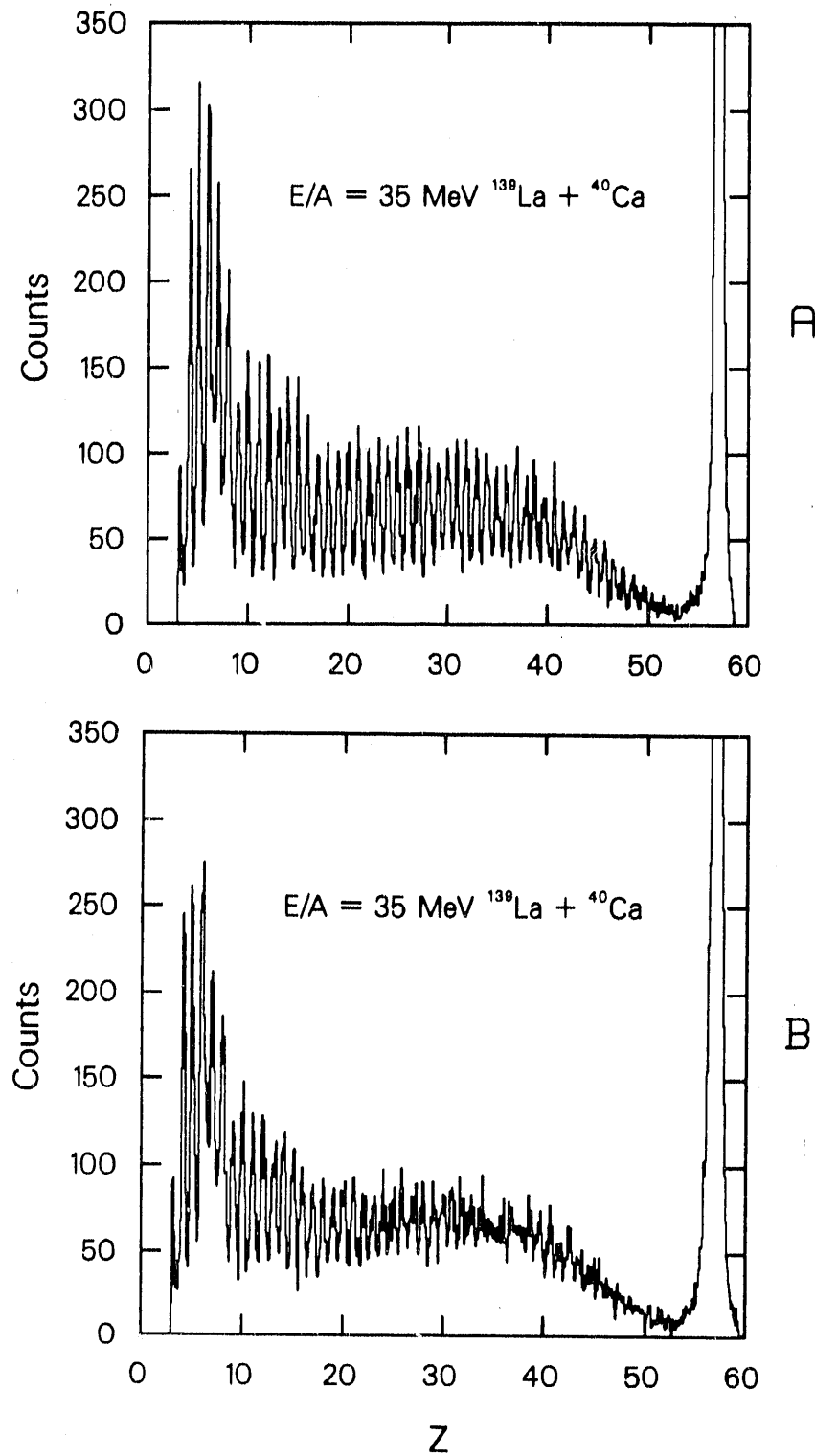


**E (5000  $\mu\text{m}$ )**

**$\Delta E$  (300  $\mu\text{m}$ )**

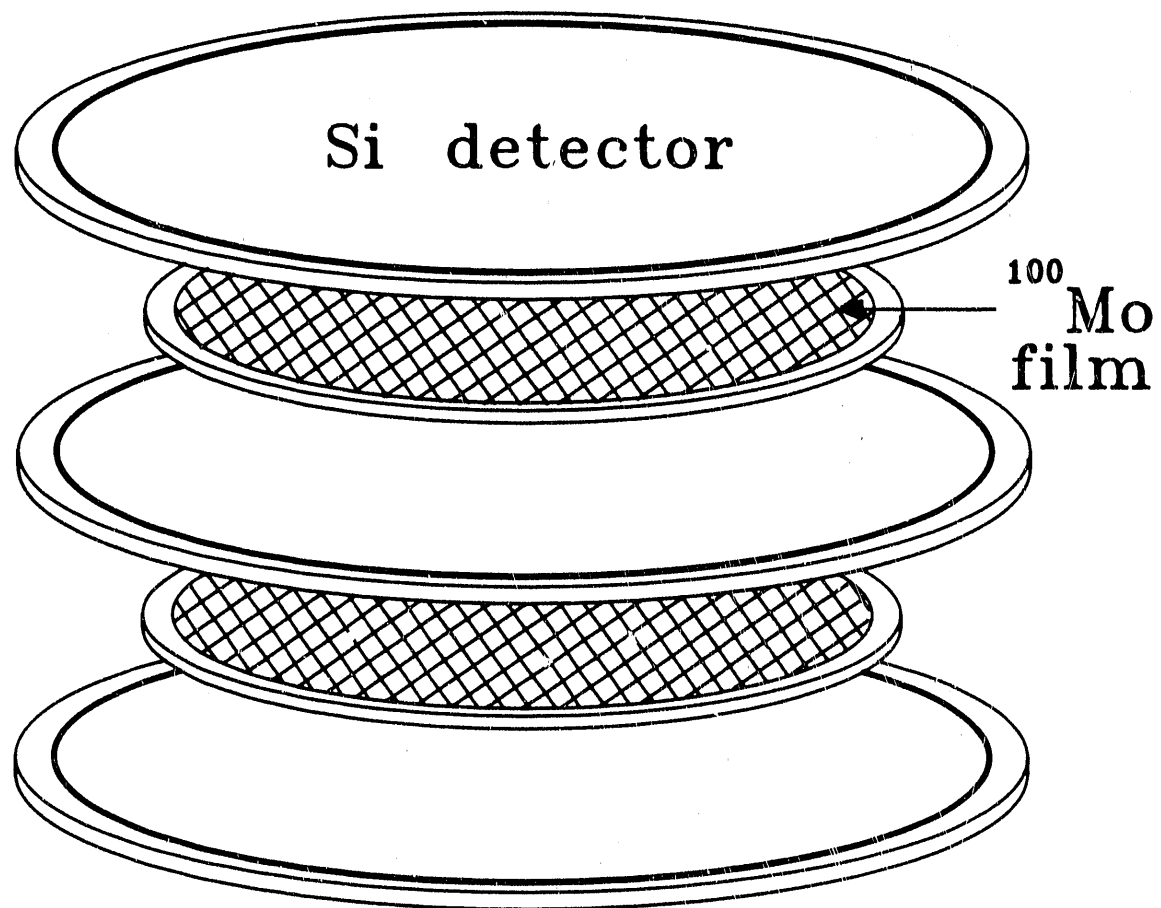
Figure 5

CBB 872-892A



XBL 8911-4001

Figure 6



XBL 9010-3445

Figure 7

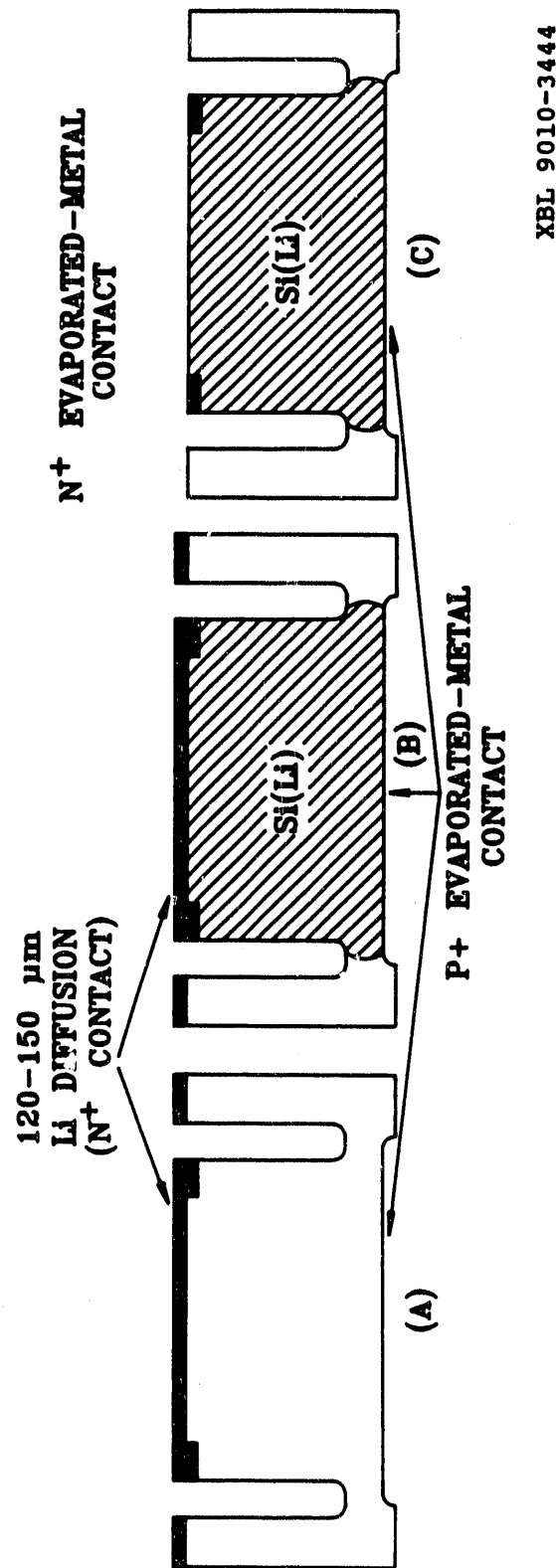


Figure 8

END

DATE  
FILMED

4/21/92

